

Improving Mechanical Properties of Maxillary Complete Dentures Through a Bioinspired Engineering Design

James A.P. White, MEng^a/Ian P. Bond, BSc, PhD^b/Daryll C. Jagger, BDS, MSc, PhD^c

Purpose: This study investigated how ribbed design features, including palatal rugae, may be used to significantly improve the structural performance of a maxillary denture under load. **Materials and Methods:** A computer-aided design model of a generic maxillary denture, incorporating various rib features, was created and imported into a finite element analysis program. The denture and ribbed features were assigned the material properties of standard denture acrylic resin, and load was applied in two different ways: the first simulating a three-point flexural bend of the posterior section and the second simulating loading of the entire palatal region. To investigate the combined use of ribbing and reinforcement, the same simulations were repeated with the ribbed features having a Young modulus two orders of magnitude greater than denture acrylic resin. For a prescribed load, total displacements of tracking nodes were compared to those of a control denture (without ribbing) to assess relative denture rigidity. **Results:** When subjected to flexural loading, an increase in rib depth was seen to result in a reduction of both the transverse displacement of the last molar and vertical displacement at the centerline. However, ribbed features assigned the material properties of denture acrylic resin require a depth that may impose on speech and bolus propulsion before significant improvements are observed. **Conclusion:** The use of ribbed features, when made from a significantly stiffer material (eg, fiber-reinforced polymer) and designed to mimic palatal rugae, offer an acceptable method of providing significant improvements in rigidity to a maxillary denture under flexural load. *Int J Prosthodont* 2011;24:589–598.

Polymethyl methacrylate (PMMA) remains the material of choice for the construction of complete dentures because of a combination of favorable properties, in particular, those of biocompatibility and excellent esthetics. However, this material is not without its limitations, which include poor mechanical strength, and further improvement would be desirable. Over the years, many attempts have been made to improve the mechanical properties of PMMA, including the incorporation of various forms of reinforcement.¹ Despite many attempts to improve the mechanical properties in terms of both flexural and impact strength, the premature failure of dentures remains an unresolved and common problem.

^aPhD Student, Department of Aerospace Engineering, Advanced Composites Centre for Innovation and Science, University of Bristol, Bristol, United Kingdom.

^bProfessor, Department of Aerospace Engineering, Advanced Composites Centre for Innovation and Science, University of Bristol, Bristol, United Kingdom.

^cProfessor, Glasgow Dental Hospital and School, University of Glasgow, Glasgow, Scotland.

Correspondence to: Mr J. White, Department of Aerospace Engineering, Advanced Composites Centre for Innovation and Science, University of Bristol, Queen's Building, University Walk, Bristol BS8 1TR, United Kingdom. Email: J.White@bristol.ac.uk

In addition to the material from which the denture is constructed, the design of the denture has a major effect on the strength and rigidity of the resultant prosthesis. The design of the denture, however, is restricted by the anatomy of the denture-bearing tissues, and dentures are generally constructed by hand using conventional techniques. More recently, the use of computer-aided design/computer-assisted manufacturing (CAD/CAM) has been suggested,²⁻⁴ but it is a technique not yet widely used for the construction of complete dentures. The use of CAD/CAM offers the possibility for the incorporation of custom-made design features that could significantly improve the performance of a denture.

A maxillary denture is, in simple terms, based on a thin plate structure design. It is widely accepted in engineering that the addition of ribs to a thin plate structure can have a significant effect on rigidity. In aerospace engineering, the external geometry of an aircraft aerofoil is determined by aerodynamic requirements; a lift-producing profile is essential. The aerofoil must be extremely light and sustain a multitude of stresses during flight, without excessive deformation. To do this, the internal geometry is used to provide adequate stiffness/weight ratio through the addition of ribs and stringers.

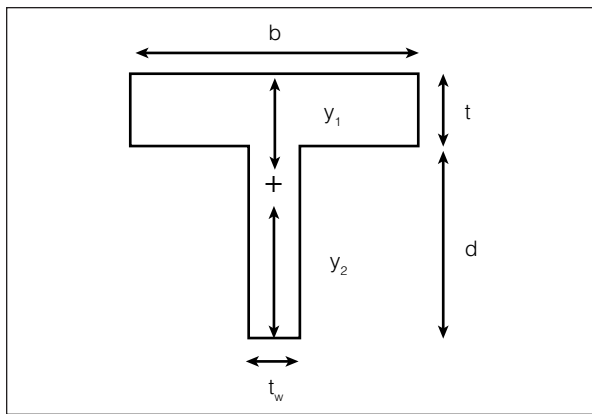


Fig 1 T-section geometry. b = span; y_1 and y_2 = distance from surface to the neutral axis (NA; NA denotes the transition line between tensile and compressive stresses in flexure); t_w = rib thickness; t = main section thickness; d = depth.

The palatal surface of a maxillary complete denture is generally left smooth so as to be acceptable to the denture wearer. However, in some circumstances, palatal rugae have been replicated in dentures to help aid patients who are struggling with aspects of speech.⁵ It is believed that surface roughness and features such as rugae provide a reference point for the tongue to establish the anterior section of the oral cavity^{6,7} and aid taste sensation.⁸ In dentistry, the literature shows that the effect of customized palatal rugae on the mechanical properties of a denture has not yet been investigated but may offer an alternative solution to improving the strength and rigidity of the denture base.

To a first approximation, palatal rugae in a denture can be viewed as a form of ribbing. This series of investigations uses finite element analysis (FEA) to demonstrate the principles of rib design and investigate the effect of the addition of palatal rugae on the rigidity of a maxillary complete denture.

FEA Studies

Effects of Increasing Second Moment of Area

The denture plate under load is often approximated experimentally to a simply supported beam subject to three-point bend flexural loading. Applying simple beam theory, it can be seen that the midpoint displacement (y) is determined by the material's Young modulus (E) and the second moment of area (I), as follows:

$$y = Pl^3 / 48EI$$

The use of reinforcement is reported to increase flexural stiffness,⁹ and hence, reduce deformation, via an increase in the Young modulus. However, a similar reduction in deformation can also be achieved by increasing the second moment of area by placing the material offset from the axis of bending by using ribbed features.

Simple beam theory was used to demonstrate the reduction in displacement and the maximum tensile stress generated in a T-section beam of varying geometry (Fig 1). The maximum tensile stress will always occur midspan on the outer surface of the beam's cross section (y_2). The beam was oriented to produce tensile stress at y_2 and compression stress at y_1 . The stress is calculated as follows:

$$\sigma = My_2 / I$$

The span (b) and cross-sectional area (A) were 10 mm and 33 mm², respectively, in accordance with ISO 20795 for testing flexural moduli. The rib thickness (t_w) and depth (d) were varied, and the main section thickness (t) was allowed to vary according to the following:

$$t = (A - dt_w) / b$$

When d or t_w are set to equal 0, the resultant geometry is that from ISO 20795.

As can be seen in Fig 2, the addition of a rib always reduces the displacement because the second moment of area increases. However, y_2 is also increasing, and, as shown in the stress calculation, the maximum tensile stress increases until increases in I begin to dominate. The most favorable rib designs will be those in the lower left region of Fig 2, which provide a reduction in displacement and a reduction in maximum tensile stress achieved.

Verification of FEA

A commercial CAD program (Autodesk Inventor 2010, Autodesk) was used to create a simple beam supported by loading pins according to the dimensions specified in ISO 20795. These were then converted to SAT files and imported into an FEA program (Abaqus/CAE 6.9-EF1, Dassault Systèmes). The load pins were

Fig 2 Carpet plot of midpoint displacement and maximum tensile stress as a function of rib depth (d) and thickness (t_w) when subject to a 25-N midspan load.

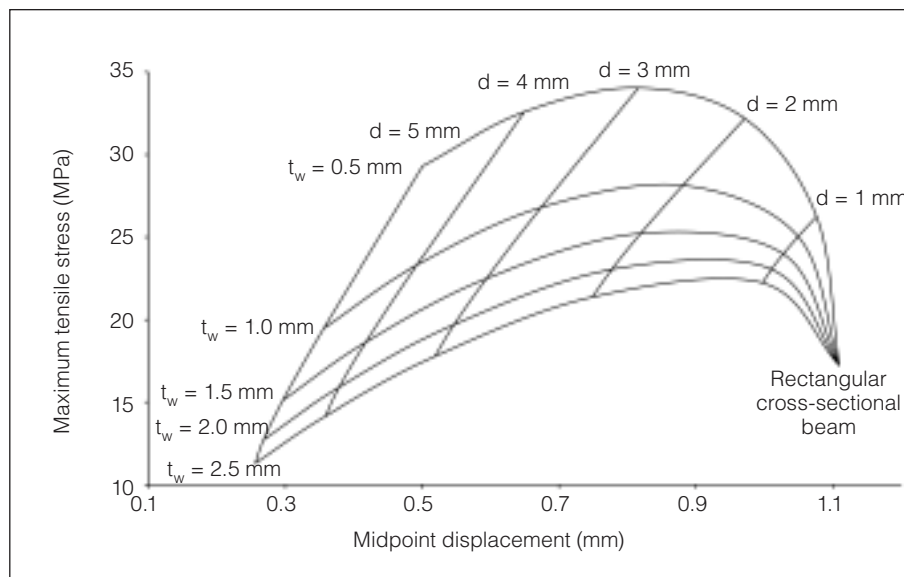


Table 1 Validation of FEA Midpoint Displacement vs Simple Beam Theory

	Coefficient of friction			
	0.1	0.01	0.001	0.0001
Theoretic displacement (mm)	1.1092	1.1092	1.1092	1.1092
FEA displacement (mm)	1.1026	1.1076	1.1081	1.1082
Error (%)	0.590	0.140	0.095	0.091

created as discrete rigid bodies, the beam as a deformable body, and all were meshed with a 0.5-mm seed size and quad-dominated elements. The beam was given a Young modulus of 1.96 GPa and a Poisson ratio of 0.3.¹⁰ The load pin geometry was designed with a 0.025-mm overclosure to prevent rigid body motion, which was resolved using the Abaqus automatic "shrink fit" option. The contact interaction between loaders and the beam used surface-surface discretization.

To validate the FEA, most notably the use of contact interactions, a comparison with simple beam theory was made for midpoint displacement. Simple beam theory applies to small deformations, and therefore, the load applied was kept minimal at 25 N. The coefficient of friction varied between 0.1 and 0.0001 and was seen to show improved agreement with the theory, as shown in Table 1.

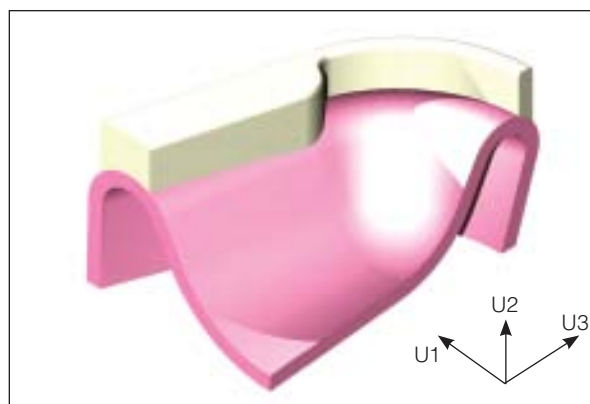


Fig 3 Control maxillary complete denture with Abaqus displacement axis.

Rib Designs Applied to a Maxillary Denture Plate

A maxillary complete denture was chosen to provide key dimensions to build a simplified denture model, as seen in Fig 3. This denture offered good symmetry around the midline and the contact area of the teeth mapped closely to a flat plane. The CAD model was approximated to straight lines and three-point arcs with a global thickness of 2 mm. The molars and incisors were approximated to solid blocks, as demonstrated diagrammatically by Nejatidanesh et al.¹¹ A half-model was used to reduce computational time of the FEA simulations.

To demonstrate the benefit of the second moment of area, five rib designs, all of equal volume (127 mm³), were created for the posterior section of the maxillary denture plate. The first rib design (RD-1) consisted of a single rib of 0.5-mm depth (equivalent

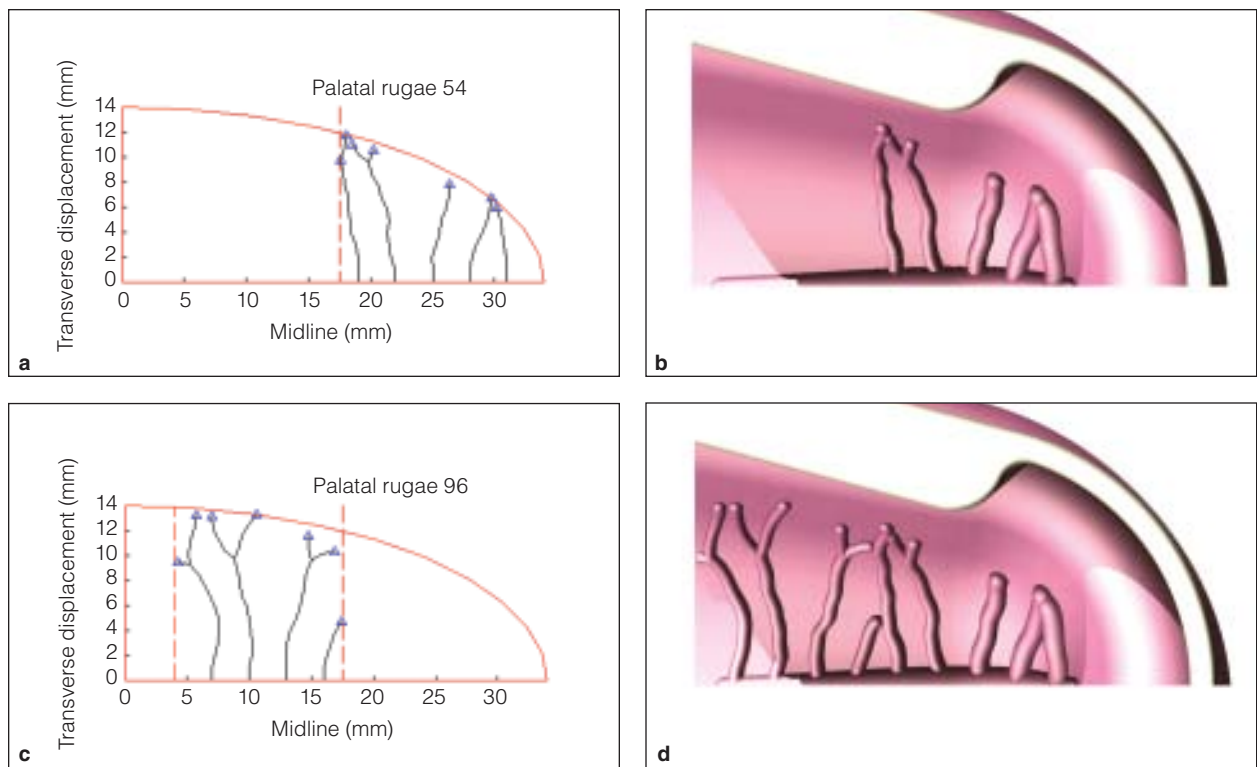


Fig 4 Geometry as drawn in Matlab and the resultant CAD models: **(a and b)** rugae in the anterior section projecting no rugae further back than the first molar; **(c and d)** extension of rugae pattern into the posterior region.

to a flat sheet), which approximates to a thickened denture base. This method was chosen as opposed to a uniform increase in the entire denture thickness since the location of additional material is important and a fair comparison between all five rib designs was intended. Subsequent rib designs consisted of four ribs of equal width housed within the same projected area, referred to as RD-1. Between the designs of RD-2 and RD-5, the rib width varied from 2.5 to 1.0 mm in 0.5-mm increments. CAD software has the ability to provide accurate volumes of parts, and thus, rib depth was varied until the volume provided lay within 1% of that of RD-1. As rib width was reduced, rib depth increased to maintain equal volume, with RD-5 having the greatest rib depth of 2.4 mm. However, such ribbing could restrict bolus propulsion and possibly interfere with speech patterns.

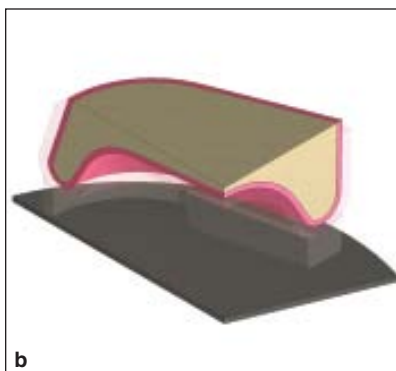
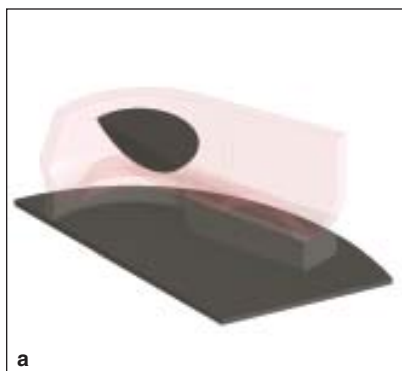
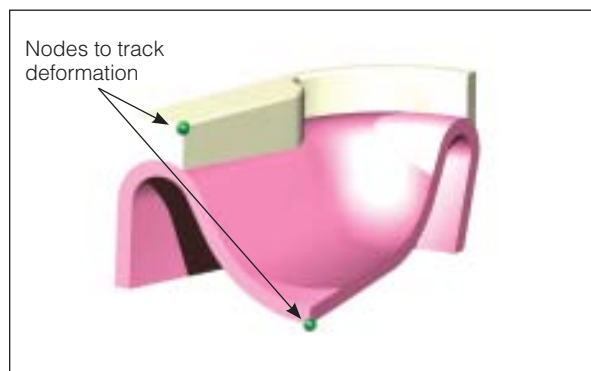
Palatal Rugae as Ribbing Features

Palatal rugae vary greatly between patients, and as such, they have been recognized as a means of forensic identification.^{12,13} It is established that rugae geometry can be curved, wavy, forked, or circular (islands)^{14,15} and are only found in the anterior region of the palate, extending no further than the first molar.^{16,17} To create bioinspired palatal rugae geometries,

a computer program (Matlab, MathWorks) was written that worked on a time-step basis, whereby rugae were “grown” a specified amount with each step from predefined origins. With each step, the growing increment could vary ± 20 degrees in growth direction, and, if the rugae achieved the length of a primary ruga (10 mm),^{15,17} they would fork. The forking angle was based on the Murray law for vascular networks and set to 75 degrees.¹⁸ The boundary in which rugae could grow was elliptical, since this simplistically describes the shape of the palatal vault, and was divided into anterior and posterior sections. The anterior section contained 5 rugae,^{15,17} with the first ruga having a depth of 1 mm and decreasing to 0.5 mm (0.125-mm increments) for the last, since rugae become less prominent toward the posterior region.¹⁷

Rugae do not naturally occur in the posterior section, but a posterior rugae pattern was created to investigate whether their addition would further improve the rigidity of the denture. After 100 program iterations, the rugae pattern producing the greatest total rugae length without any intersections was chosen. The Matlab program produces a text file of point data that can be imported into Autodesk Inventor 2010. From the two-dimensional (2D) pattern this produces, 3D projections were made onto the palatal vault, which acted as centerline rails for semicircular

Fig 5 (right) Nodes placed on the posteriormost point of the centerline and inside corner of the last molar to track deformations of the denture under load.



Figs 6a and 6b Assemblies of (a) LP-1 and (b) LP-2, as modeled in Autodesk Inventor.

Fig 6c Imported geometry of LP-1 meshed in Abaqus/CAE 6.9-EF1.

cross-sectional lofts, as shown in Fig 4. All posterior rugae were maintained at a depth of 0.5 mm. A generic raphe, a ridge of tissue occurring along the centerline of the palate, was created with similar dimensions to that of the rugae, with 1-mm and 0.5-mm depths in the anterior and posterior sections, respectively. The anterior rugae and raphe total a volume of 55 mm³, and the posterior rugae a further 23 mm³. Again, to ensure fair comparison with a thickened denture, two sheets of equal volume to the anterior and posterior rugae that encompassed the same projected area were created. Since the majority of the raphe volume is within the anterior section, the total contribution to volume was included in the anterior sheet only.

The CAD-generated denture and respective rib designs were converted to SAT files and imported into the FEA as deformable bodies. Partitioning was used to allow the parts to be meshed using swept quad solid elements. Element size sensitivity checks deemed a 0.6-mm seed size for meshing the denture able to provide accurate results without unnecessary computation. To help reduce discretization error in reinforcement volumes without incurring excessive analysis time, the ribbing features were meshed with a 0.3-mm seed size. Because of the complexity of the rugae geometries, these could only be meshed using tetrahedral solid elements. A tied constraint was

established between the denture and the rib feature using surface-surface discretization. Node sets were created on the inside corner of the last molar and on the posterior centerline to track deformations (Fig 5).

Using the same CAD program, the geometry of test equipment adapted from Tsue et al¹⁹ was created and also imported into the FEA software (Fig 6). This consisted of a flat bed in contact with the base of the teeth and a spheric loading pin of 25-mm diameter applied to the central section of the palatal side of the denture. This approach to testing complete dentures, where the load point or reaction surface has been localized to the midline of the denture palatal side, has been used elsewhere to approximate the torus palatinus being the load-bearing surface.²⁰ By loading the denture in this manner, the posterior section of the denture plate experiences three-point bending. This method of loading the denture was referred to as load pin 1 (LP-1). To investigate whether the method of loading a complete denture has a significant effect on the deformation shape, a loading pin conforming to the entire palatal surface, with the properties of bone and mucosa, was also modeled. This form of loading was referred to as load pin 2 (LP-2). The flat plate and spheric loader were imported into the FEA program as discrete rigid bodies and meshed with quad shell elements and a 0.6-mm mesh seed size. The Young

Table 2 Reduction in Displacement of Tracking Nodes for RD-1 to RD-5 Relative to Those of the Control Denture (No Ribbing) for LP-1

Modulus (GPa)	Center (U2, %)	Molar (U1, %)
RD-1		
1.96	20.9	15.6
19.6	41.9	36.8
196	53.0	47.9
RD-2		
1.96	26.0	20.4
19.6	49.8	45.2
196	66.9	61.5
RD-3		
1.96	29.1	23.5
19.6	54.4	49.8
196	73.1	67.4
RD-4		
1.96	34.6	28.9
19.6	61.5	56.7
196	79.8	73.6
RD-5		
1.96	45.8	39.6
19.6	72.2	66.7
196	85.8	78.8

moduli of the denture base and acrylic resin teeth were 1.96 GPa and 2.94 GPa, respectively.¹⁰ For LP-2, the Young moduli of bone and mucosa were 13.5 GPa and 0.98 MPa, respectively.¹⁰ All deformable parts were given a Poisson ratio of 0.3.¹⁰ The additional ribbing was given an initial modulus value equivalent to denture base acrylic resin. A further possible development that may lead to improvements by combining rib design with material reinforcement (eg, addition of glass fibers or steel wire) was also investigated by implementing a two order of magnitude increase in Young modulus (to 196 GPa) for the rib features. This increased modulus value is similar to that of steel, which has previously been investigated as a reinforcement material.¹ The use of a high-modulus reinforcement was a subsidiary reason for choosing the geometry of RD-1 to be represented as a flat sheet. The poor wetting characteristics of powder/liquid denture acrylic resin mean that fiber reinforcements such as E-glass can only be incorporated using alternative biocompatible resins (eg, bisphenol glycidyl methacrylate [bis-GMA], triethylene glycol dimethacrylate [TEGDMA]).^{9,19} Thus, these fiber-reinforced composite layers can then only be integrated into denture base acrylic resin as discrete sheets.

The same contact interactions were used for these FEA studies of a complete maxillary denture as for the flexural beam example with a coefficient of friction for tangential contact of the load points of 0.1.²¹ The load applied to the dentures was 110 N (55 N for the half model), a typical chewing load for an edentulous patient.²²

Results

LP-1

Rib Designs 1 to 5. Comparing the decreasing U1 displacements (see Fig 3) of the last molar (moving away from the midline plane) between RD-1 to RD-5 in Table 2 clearly demonstrates that, in bending, the consequential increase in second moment of area through greater rib depth causes an increase in overall rigidity. It can also be seen that ribs of materials with higher moduli yield significant improvements. A similar trend is also seen for the U2 displacement (see Fig 3) of the center node (moving toward the flat bed).

As the modulus of the reinforcing ribs is increased, the rate of decrease in displacement is reduced. The use of tied constraints in all models is equivalent to the ribs being perfectly bonded to the denture plate, and thus, the ribs are loaded through shear stress. Therefore, as the stiffness mismatch increases, the full potential of the ribbing cannot be realized. Figure 7 shows the shear stresses generated in the denture plate as the load is transferred to the ribbing.

It is important to note that when the ribbing has the same modulus as denture acrylic resin, the shear stress patterns are relatively uniform and do not appear to be influenced strongly by the termination points of the ribs (Fig 7a). However, when the Young modulus of the rib material is increased by two orders of magnitude, the large change in stiffness gives rise to stress concentrations shown most notably on the two posterior ribs (red, Fig 7b). The use of high-modulus reinforcement and the resultant stiffness mismatch has previously been recognized as a cause of stress concentrations.^{1,23} In the case of a high-modulus material used for the ribbing, the majority of the displacement is likely to occur in the unreinforced section of the denture.

In the control denture, the bending moment can only be reacted via tensile and compressive stresses within the 2-mm-thick base plate, and because of the low modulus, the deformation (or strain) is high to be able to reflect the required magnitude of stress (Fig 8a). In RD-5, with acrylic resin denture base properties, the peak tensile stress (blue) is now seen to occupy only the outermost section of the ribs, and

Fig 7 (right) LP-1 shear stresses created in RD-5. **(a)** Ribbing of acrylic resin denture base; **(b)** Ribbing of modulus 196 GPa. Ribs were removed for clarity.

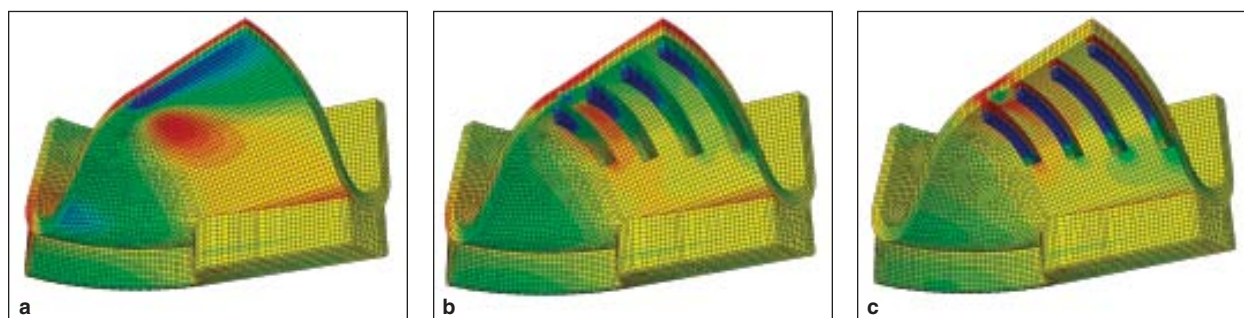
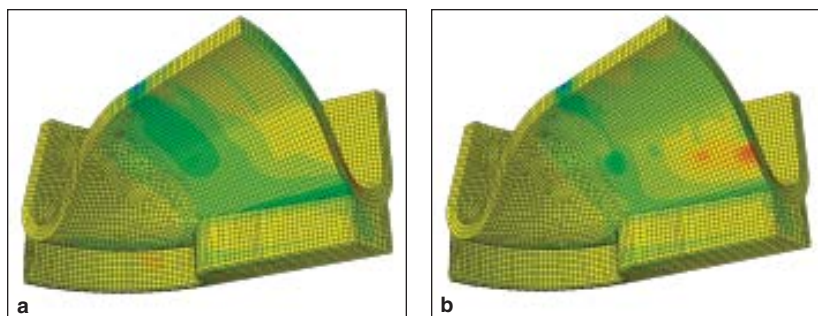


Fig 8 LP-1 normal stress. Blue and red denote tension and compression, respectively: **(a)** control; **(b)** RD-5 with properties of acrylic resin denture base; **(c)** RD-5 with a modulus of 196 GPa.

the counteracting compressive stress remains in the denture base plate (Fig 8b). The maximum tensile stress within the ribbing is also slightly higher than that of the control denture, as demonstrated in Fig 2. Increasing the rib material modulus to 196 GPa sees the bending moment reacted via stresses contained entirely in the ribbing (Fig 8c). Furthermore, because the rib cross-sectional area is small, these stresses are larger than found in the control. However, this is mitigated by the fact that a greater material stiffness is generally associated with greater strength. Despite higher shear stresses occurring, the tensile and compressive stresses within the posterior section of the denture base have been reduced. This reduction in global stress as a result of reinforcement bearing the majority of loading has been hypothesized previously.²³

Palatal Rugae. Unlike RD-1 to RD-5, the palatal rugae occupy the anterior section of the denture where there is complex curvature, and the loading of this area is therefore more complex than the posterior section. For reinforcement moduli of 1.96 GPa and 19.6 GPa, a thickened denture base equivalent is seen to provide fractionally more rigidity than the rugae. However, with rugae of material stiffness equivalent to 196 GPa, they provide a greater reduction in center and molar displacements. Combining anterior rugae with posterior rugae, as found in designs RD-1 to RD-5, the tracking node displacements were found to be smaller than a thickened denture for all modulus

Table 3 Reduction in Displacement of Tracking Nodes for Palatal Rugae Relative to Those of the Control Denture (No Ribbing) for LP-1

Modulus (GPa)	Center (U2, %)	Molar (U1, %)
Anterior rugae + raphe		
1.96	5.7	3.8
19.6	16.8	11.8
196	31.5	24.6
Anterior rugae + raphe equivalent sheet		
1.96	6.4	4.9
19.6	17.7	14.6
196	25.0	21.5
Anterior and posterior rugae + raphe		
1.96	11.2	7.4
19.6	34.1	26.1
196	53.0	45.8
Anterior and posterior rugae + raphe equivalent sheet		
1.96	10.2	7.4
19.6	30.8	25.0
196	43.7	39.1

values (Table 3). With the volume of rugae being lower than RD-1 to RD-5, it is to be expected that the percentage reductions in center and molar displacements would be smaller.

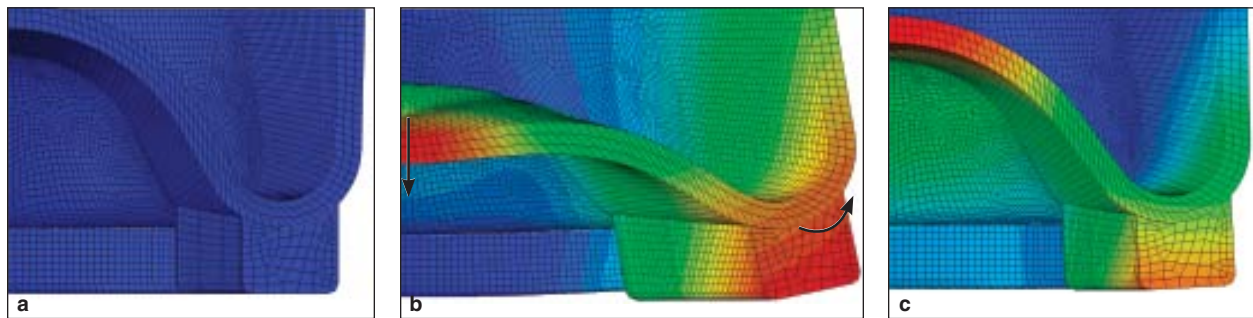


Fig 9 (a) Undeformed control denture; (b) deformed control denture with LP-1; (c) deformed control denture with LP-2 (negligible deformation). Color contours denote combined displacement magnitude. Deformation scale factor is 20 for both b and c.

Table 4 Reduction in Displacement of Tracking Nodes for RD-1 to RD-5 Relative to Those of the Control Denture (No Ribbing) for LP-2

Modulus (GPa)	Center (U2, %)	Molar (U1, %)
RD-1		
1.96	0.2	0.7
19.6	1.4	2.3
196	5.7	5.4
RD-2		
1.96	0.3	1.3
19.6	2.3	4.2
196	12.2	11.2
RD-3		
1.96	0.4	1.8
19.6	3.5	5.7
196	16.9	14.8
RD-4		
1.96	0.8	2.8
19.6	6.0	8.4
196	23.7	19.5
RD-5		
1.96	2.6	5.1
19.6	12.2	13.6
196	33.2	25.2

Table 5 Reduction in Displacement of Tracking Nodes for Palatal Rugae Relative to Those of the Control Denture (No Ribbing) for LP-2

Modulus (GPa)	Center (U2, %)	Molar (U1, %)
Anterior rugae + raphe		
1.96	0.0	0.0
19.6	-0.4	0.0
196	0.3	1.2
Anterior rugae + raphe equivalent sheet		
1.96	-0.1	-0.1
19.6	-0.3	-0.2
196	-0.1	0.0
Anterior and posterior rugae + raphe		
1.96	0.0	0.2
19.6	0.0	0.9
196	2.8	4.0
Anterior and posterior rugae + raphe equivalent sheet		
1.96	0.0	0.0
19.6	0.0	0.4
196	1.0	1.5

LP-2

Rib Designs 1 to 5. Simulating a close-fitting denture, LP-2 places much greater constraint on the allowable deformation of the denture during loading. The flexibility of the mucosa does facilitate some movement, and the directions traveled by the tracking nodes are similar to those with LP-1, but the displacement values are nearly an order of magnitude lower. Comparisons between the deformation shape

for LP-1 and LP-2 are shown in Fig 9. Nonetheless, the same trends in increasing rigidity demonstrated with LP-1 are observed, albeit with smaller margins (Table 4).

Palatal Rugae. It was expected that the rugae would provide the same general trends as found for LP-1, but this was not the case. Changes in displacement were negligible and, in some cases, displacements increased (denoted by a negative percentage). The exception to this was the use of anterior and

posterior rugae and a Young modulus value of 196 GPa (Table 5). The use of node tracking is a crude measure of component rigidity, particularly when the deformation shape is unknown. For simple three-point flexural loading, it was expected that the molars would move outward and that the arc of the posterior denture would effectively flatten. As demonstrated for LP-1, this was the overall deformation shape, and the recorded displacements indicated ribbing to be beneficial. More complex deformation under LP-2 loading, attributed to design features that increase local stiffness and a high level of constraint, may not be adequately captured using this technique.

Discussion

The FEA simulations presented herein are simplistic in their approach. However, they demonstrate the potentially significant advantages that could be gained from the addition of rib features to the basic structural design of the denture under certain loading cases. They also show differences between experimental and simulated *in vivo* methods of loading complete dentures. Further research needs to be invested into understanding the exact loading of dental components to allow optimal design. Current research on automated, biologically inspired oral simulators may provide the ability to complete such studies.²⁴

Computer-aided engineering prior to the final fabrication of a denture could allow numerous variations in design to be simulated and optimized using FEA.²⁵ For example, Kelly²⁶ recognized that localized thinning of the denture base resulting from rugae depressions on the palatal side act as fatigue initiation sites. Transposing the exact replication of patient rugae (or an optimized combination of naturally occurring and synthetic rugae) to maintain uniform thickness may alleviate this as a source of failure. Though methods for replicating rugae using traditional wax techniques and plaster casts have been successfully applied,⁵ the accuracy of the method is questionable. However, the adaptation of the tailored CAD software and rapid prototype tooling of Sun et al³ used to replace lost wax plaster casting may provide a viable alternative. Selective laser sintering has been used to create partial denture frameworks²⁷ and could produce high modulus features such as rugae. Derived from the same CAD geometry, these inserts would fit accurately inside the rapid prototyping tooling. Although the initial investment for implementing new technologies may be high, over time, it can yield reduction in overall costs, particularly through reduced labor of the dental technician.^{25,28}

Conclusions

The use of tailored ribbing on a denture can provide a reduction in deformation under flexural loading. When the ribbing is made from a baseline denture acrylic resin material and is below a certain dimensional threshold, it offers little improvement compared to a thickened base plate. However, the use of a bioinspired design to increase the second moment of area combined with the use of higher-modulus materials can potentially yield significant increases in rigidity. The use of rugae and posterior rugae-like projections appears to provide an acceptable means of achieving integral ribbed features.

Acknowledgments

This study was funded by a University of Bristol Postgraduate Scholarship.

References

1. Jagger DC, Harrison A, Jandt KD. The reinforcement of dentures. *J Oral Rehabil* 1999;26:185–194.
2. Kawahata N, Ono H, Nishi Y, Hamano T, Nagaoka E. Trial of duplication procedure for complete dentures by CAD/CAM. *J Oral Rehabil* 1997;24:540–548.
3. Sun Y, Lü P, Wang Y. Study on CAD&RP for removable complete denture. *Comput Methods Programs Biomed* 2009;93:266–272.
4. Maeda Y, Minoura M, Tsutsumi S, Okada M, Nokubi T. A CAD/CAM system for removable denture. Part 1: Fabrication of complete dentures. *Int J Prosthodont* 1994;7:17–21.
5. Gitto CA, Esposito SJ, Draper JM. A simple method of adding palatal rugae to a complete denture. *J Prosthet Dent* 1999;81:237–239.
6. Erb DP. Speech effects of the maxillary retainer. *Angle Orthod* 1967;37:298–303.
7. Kong HJ, Hansen CA. Customizing palatal contours of a denture to improve speech intelligibility. *J Prosthet Dent* 2008;99:243–248.
8. Steas AD. Overcoming altered taste sensation in complete denture wearers. *J Prosthet Dent* 1997;77:453.
9. Narva KK, Lassila LV, Vallittu PK. The static strength and modulus of fiber reinforced denture base polymer. *Dent Mater* 2005;21:421–428.
10. Ates M, Cilingir A, Sülün T, Sünbuloğlu E, Bozdağ E. The effect of occlusal contact localization on the stress distribution in complete maxillary denture. *J Oral Rehabil* 2006;33:509–513.
11. Nejatidanesh F, Peimannia E, Savabi O. Effect of labial frenum notch size and palatal vault depth on stress concentration in maxillary complete dentures: A finite element study. *J Contemp Dent Pract* 2009;10:59–66.
12. Hermosilla VV, San Pedro VJ, Cantin LM, Suazo GIC. Palatal rugae: Systematic analysis of its shape and dimensions for use in human identification. *Int J Morphol* 2009;27:819–825.
13. Filho IEM, Sales-Peres SHC, Sales-Peres A, Carvalho SPM. Palatal rugae patterns as bioindicators of identification in forensic dentistry. *RFO* 2009;14:227–233.

14. Hauser G, Daponte A, Roberts MJ. Palatal rugae. *J Anat* 1989; 165:237-249.
15. Kapali S, Townsend G, Richards L, Parish T. Palatal rugae patterns in Australian aborigines and Caucasians. *Aust Dent J* 1997;42:129-133.
16. Allen H. The Palatal rugae in man. *Acad Nat Sci* 1888;40: 254-272.
17. Patil MS, Patil SB, Acharya AB. Palatine rugae and their significance in clinical dentistry: A review of the literature. *J Am Dent Assoc* 2008;139:1471-1478.
18. Murray CD. The physiological principle of minimum work applied to the angle of branching of arteries. *J Gen Physiol* 1926; 9:835-841.
19. Tsue F, Takahashi Y, Shimizu H. Reinforcing effect of glass-fiber-reinforced composite on flexural strength at the proportional limit of denture base resin. *Acta Odontol Scand* 2007; 65:141-148.
20. Vallittu PK, Lassila VP, Lappalainen R. Transverse strength and fatigue of denture acrylic-glass fiber composite. *Dent Mater* 1994;10:116-121.
21. Kibi M, Ono T, Dong J, Mitta K, Gonda T, Maeda Y. Development of an RPD CAD system with finite element stress analysis. *J Oral Rehabil* 2009;36:442-450.
22. Prombonas AE, Vlissidis DS. Comparison of the midline stress fields in maxillary and mandibular complete dentures: A pilot study. *J Prosthet Dent* 2006;95:63-70.
23. Tomoyuki I, Hajime S, Noriyuki W, Takashi O. Effect of cross section shape of metal strengthener on stress distribution in acrylic denture bases. *Prosthodont Res Pract* 2004;3:1-7.
24. Raabe D, Alemzadeh K, Harrison AJL, Ireland AJ. The chewing robot: A new biologically-inspired way to evaluate dental restorative materials. Presented at the 31st annual International Conference of the IEEE Engineering in Medicine and Biology Society, Minneapolis, 2-6 Sept 2009, 2009:6050-6053.
25. Chang CC, Lee MY, Wang SH. Digital denture manufacturing—An integrated technologies of abrasive computer tomography, CNC machining and rapid prototyping. *Int J Adv Manuf Technol* 2006;31:41-49.
26. Kelly E. Fatigue failure in denture base polymers. *J Prosthet Dent* 1969;21:257-266.
27. Bibb R, Eggbeer D. Rapid manufacture of removable partial denture frameworks. *Rapid Prototyp J* 2006;12:95-99.
28. Liu Q, Ming CL, Schmitt SM. Rapid prototyping in dentistry: Technology and application. *Int J Adv Manuf Technol* 2006; 29:317-335.

Copyright of International Journal of Prosthodontics is the property of Quintessence Publishing Company Inc. and its content may not be copied or emailed to multiple sites or posted to a listserv without the copyright holder's express written permission. However, users may print, download, or email articles for individual use.